

# Offshore Wind Farms Energy Injection in the Electrical Grid - Lithium Battery to Mitigate Power Fluctuations

Djamel Ikni, Mamadou Bailo Camara, Brayima Dakyo

Electrotechnic and Automatic Research Laboratory of Le Havre (GREAH) University of Le Havre, 75 rue Bellot, 76600 Le Havre –France

(djamel.ikni@univ-lehavre.fr, camaram@univ-lehavre.fr, brayima.dakyo@univ-lehavre.fr)

‡ Corresponding Author; Djamel Ikni, 75 rue Bellot, 76600 Le Havre –France, Tel: + 3302 32 85 99 00  
djamel.ikni@univ-lehavre.fr

*Received: 18.07.2015 Accepted: 03.09.2015*

**Abstract-** The wind farm energy injection in the electrical grid generates the economic and technical challenges which must to be solved for successful large scale wind energy integration in electrical grids. Due to wind speed variations, the wind farm output power presents the fluctuating components which are not compatible to the electrical grid requirements. Today, this problem is a major challenge with the wind farm projects increasing in the world. Large power variations cause the deviations of rms voltage and the frequency compared to nominal values in point of the coupling. These deviations cause generally the protective equipment activation which causes a disconnection of wind farms from the grid. To avoid these problems, the electrical grid managers use the grid code requirements to regulate the wind energy injection process in the grid. Using energy storage devices such as a lithium battery or ultracapacitors to compensate the power fluctuations from wind farm is an interesting solution. This paper deals this issue to improve the injected energy in electrical grid by the wind farm using lithium battery. Proposed approach allows compensating the wind energy fluctuations, so that the energy destined to electrical grid becomes compatible to electrical grid code requirements. Studied system configuration includes a wind farm with rated power of 300MW, a lithium battery module with a maximum power of 30MW and electrical grid. Lithium battery is connected to grid through an inverter and the power fluctuations from wind farm are assigned to battery. To show the performances of the control strategy, some simulation results are presented and analyzed using Matlab/SimPowerSystem software.

**Keywords** Offshore wind farm, power fluctuation, power smoothing control, energy storage unit.

## 1. Introduction

Although advantages of wind energy in terms of ecological issue are significant, the technical challenges to integrate the energy from wind farms in electrical grids are major. The impact of wind speed variations on the electrical grid performances are the source for many technical issues which must be compensated to increase a development of wind farms connected to grid. In the case of large scale wind farm integration, power fluctuations can cause electrical grid performances degradation in point of coupling, such as the deviations of voltage and frequency compared to rated values. In more, the random behavior of wind speed causes the difficulties in power system operation planning and optimal control of the system. Frequency and voltage variations can also be significant in cases when wind turbines

are connected to an electrical grid [1]. In other terms, the main characteristics of wind power that must be analyzed to understand their impact on the conduct and stability of the electrical grid are the fluctuations and uncertainty on production. The unpredictable nature of wind induces an uncertainty in wind generation.

Due to these problems associated to wind energy integration in grid, the electrical grid managers have developed the technical requirements implemented in “grid-code” which must to be respected for wind farm connection to grid [2]. In [3], the standard deviation of forecasts / achievements in France is 3% to maturity of one hour and 7% to maturity of 72 hours, which is quite satisfactory for the control of the supply-demand balance. This result can be better for the case of offshore, because the wind is less

turbulent, [4], [5]. For the fluctuating nature of wind generation, the rate of production beyond which the output fluctuations become very complex to manage, is estimated about 30% of the total power of the electrical grid, [6]. These fluctuations have a threshold imposed by electrical grid managers in the grid codes, [7] and [8]. In 2013, wind power has reached a critical size in relation to the total power in three European countries [9]. In Denmark; the installed capacity is 3.1 GW, which presents 24.4% of the total capacity of the power grid. In Germany, the installed capacity is 20 GW; or 14.8% of total electrical grid capacity. In Spain, the installed capacity is 11 GW corresponding to 14.1% of the total capacity of the power grid.

To avoid the slowing or limit the rate of integration of wind power into the grid. The integration of storage units to absorb the fluctuations of the power produced by an offshore wind farm is an appropriate solution; this is due to technological advances in the field of storage. The objective of this paper is to determine the storage units which must to be associated with the offshore wind farm to smooth the power injected to the grid. The first step of this study is the classification of storage units according the performances that can bring to the wind farm to improve the quality of injected energy in grid. The second step is to define a methodology to facilitate the choice of storage units. The third stage is devoted to developing the models and control algorithms for system energy management.

**2. Energy storage devices classification based on their performances**

**Table 1.** Energy storage devices classification according to services that can offer to the wind farm applications.

Technology \ Service	Sodium sulphur	Flow battery	Lithium Ion	Supercapacitor	Lead Acid	Pumped-Hydro	CAES	SMES	Flywheel ES	Ni-Cd	Zebra
Forecast improvement											
Inertia											
Production smoothing											
Grid frequency support											
Voltage control support											
LVRT											
Black start											
Storage arbitrage											
Production levelling											
Primary reserve											
Secondary reserve											
Tertiary reserve											

There are many storage devices in market, but their effectiveness depends on the conditions of exploitation and implementation ease. The classification of energy storage for renewable energy applications in general, and in the wind

energy sector in particular, is an essential step. This classification according to their performances facilitates the choice of energy storage device which must be used to mitigate the wind farm energy fluctuations. The classification of energy storage devices according to the services that can offer to wind farms are shown in Table 1 [10].

This classification is based on the intermittent nature of wind power, the grid code requirements and the role of energy storage devices in the goal to consider the wind farm as a conventional energy source. For example, an association of long-term energy storage devices or that of medium term with the wind farm can reduce the forecasting error impact for wind generation, so increasing its rate of integration to the grid and minimize the penalties. The energy storage devices which are more adapted for this mission are: the flywheel, the superconducting, the ultracapacitors and the batteries.

**3. Wind distribution modeling for wind farm**

A critical point in the wind farm study is the wind distribution modeling in wind farm [11]. Many models have been developed in order to get his actual behavior, but these models are complex, [12] and [13]. The proposed model in this paper takes into account the inequality repartition of the wind speed in the wind farm. This distribution is due to strong interactions between wind speed and turbines positioned in first sectors in direction of wind speed. These interactions cause wake effects which are considered in the proposed model. In [14] and [15], a simplified representation of wake effect is presented. In this last one, the speed of the wind diminished about 2-4% after each row/column of the farm. The same approach is used in proposed model for wind distribution in wind farm. Also, to reflect the wind speed delay in the spread between the wind turbines, a delay function is added in wind speed model.

In [16] and [6], the authors have shown that when the wind direction is perpendicular to the lines of the wind farm, the produced power from wind farm presents more fluctuations. This worst case is considered with an assumption that the wind speed is same for all wind turbines positioned in same line. The wind speed model for *i* line is presented in (1), where *dt<sub>i</sub>* is the delay function, and *ds<sub>i</sub>* presents the wake effect. These parameters depend on the wind farm configuration. This configuration is fashioned so as to maximize production and minimize the turbulence caused by the downstream turbines to in those upstream.

$$v_i = v_1(t + dt_i) (1 - ds_i) \tag{1}$$

For this raison, an optimum distance between wind turbines is necessary as described in [12] and [17]. This distance is about 7 times of wind turbine’s diameter.

Figure 1 shows the configuration of the wind farm with power rated of 300MW. This power is produced from 60 Permanent Magnet Synchronous Generators (PMSG) linked to turbines. These generators are distributed in 10 lines, and each line includes 6 wind turbines which are in the same sector and submitted to similar wind speed.

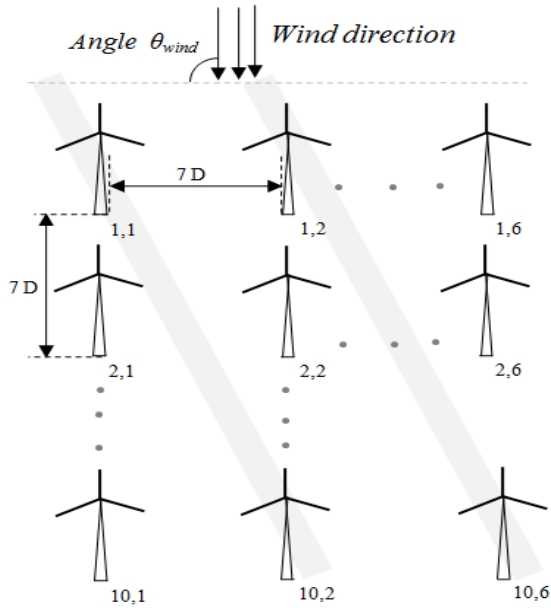


**Fig. 1.** Wind turbines positions in offshore wind farm.

The power produced by wind farm is the sum of the contributions of all turbines. These contributions are related to wind speeds profiles applied to each turbine. For this reason, it is necessary to calculate  $d_{ti}$  and  $d_{si}$  parameters as expressions in (2) and (3), respectively.

$$dt_i = \frac{7 \cdot D}{v_{1mean}} \cdot i \tag{2}$$

$$ds_i = b \cdot i \tag{3}$$

In these equations,  $v_{1mean}$  is the average value of the wind speed for first line ( $i=1$ ),  $D$  presents the wind turbine diameter, and  $b$  is between 2% and 4%. In this paper  $b$  is fixed to 2%.

Using (2) and (3) in (1), the wind speed profile for each wind turbine can be estimated as presented in (4).

$$v_i = v_1 \left( t + \frac{7 \cdot D}{v_{1mean}} \cdot i \right) \cdot (1 - b \cdot i) \tag{4}$$

Total power generated by the wind farm is given by the following equation:

$$P_i = \begin{cases} \frac{1}{2} \rho \pi R^2 C_{pmax} v_i^3 & v_i \leq 11,5 m/s \\ 5MW & v_i > 11,5 m/s \end{cases} \tag{5}$$

**6.1. Wind speed model evaluation**

To evaluate the wind speed model, the wind speed profile for first line turbines presented in Fig.2 is used. Average value of this profile is about 10.05 m/s with the fluctuations of  $\pm 15\%$ .

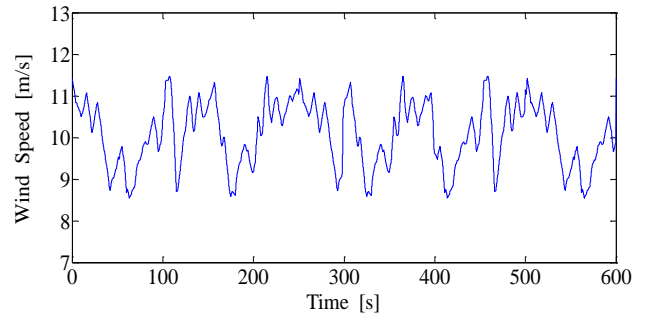


**Fig. 2.** Wind speed profile  $V_1$  for first line turbines.

The wind speed model evaluation approach is based on a comparison between wind farm power fluctuations with those extracted in real applications described in [18] and [19]. To quantify power fluctuations, used method is based on the spectrum analysis of powers plotted in Fig.3. The obtained specters from computed power ( $P_{model}$ ) and reference ones ( $P_{ref}$ ) are illustrated in Fig.4. The comparison criterion is based on an analysis of Fluctuation Harmonic Content (FHC) parameter. This last one is same to Normalized Standard Deviation (NSD) of the power in time domain described in [6]. FHC parameter can be estimated using (6), where  $P_0$  is the produced power average value for 10 minutes,  $F$  presents the frequency interval. In this equation  $P(f)$  correspond to spectrum analysis of power using Fast Fourier Transform (FFT).

$$FHC(F) = \frac{\sqrt{\sum_{f \in \{F\}} \left( \frac{P(f)}{\sqrt{2}} \right)^2}}{P_0} \tag{6}$$

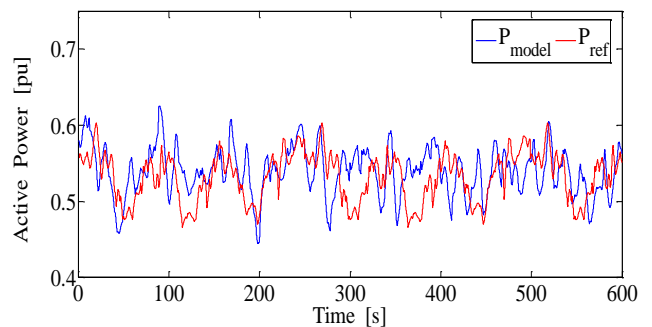


**Fig. 3.** Computed power compared  $P_{model}$  to measured power in real application  $P_{ref}$ .

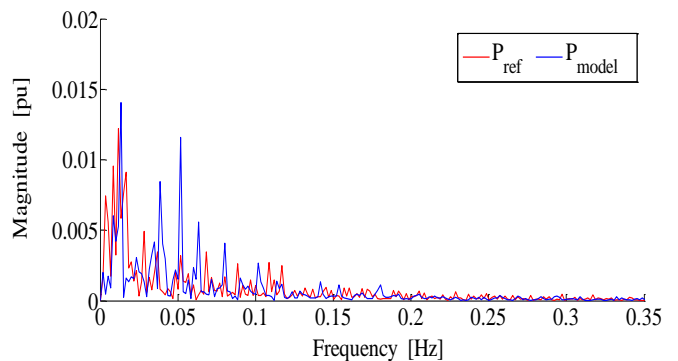


**Fig. 4.** Spectrum analysis of computed power and reference ones.

The spectrum of each power is divided into three frequency domain: - First domain is based on low frequencies which are lower than 10 mHz. - The second concerns the medium frequencies which are between 10 to 300 mHz. -The last zone corresponds to high frequencies which are above 300 mHz. FHC parameters estimated for Pref and Pmodel are summarized in Table 2.

**Table 2.** FHC parameters estimated for Pref and Pmodel

frequency region	f < 0.01Hz	f ∈ [0.01-0.3Hz]	f > 0.3Hz	full region
FHC of Pref	2.145	2.37	0.035	4.32
FHC of Pmodel	2.18	2.4	0.02	4.44

Estimated values of FHC in each zone are same. The FHC values corresponding to high frequencies domain are negligible for two powers. For medium frequencies domain, FHC is about 2.37% for Pref, and 2.4% for Pmodel which presents a difference of 0.03%. In the case of low frequencies domain, the values of FHC are 2.145% for Pref, and 2.18% for Pmodel which correspond a difference of 0.035%. These differences are very small, it allows to validating the proposed distribution model of the wind speed for wind farm application.

**4. Energy quality compatibility problems between wind farm production and grid code requirements**

To show the wind farm power fluctuations impact on the electrical grid frequency, the system configuration presented in Fig.5 is studied. In this case, the offshore wind farm and a diesel power plant are connected to a purely resistive load, and the wind farm contribution is 20% of total production. The diesel unit includes an excited synchronous generator and diesel engine. The synchronous generator is modeled as a fifth-order model [20]. The diesel engine model is given in [21] and [22]. Used parameters in this simulation are given in the appendix section.

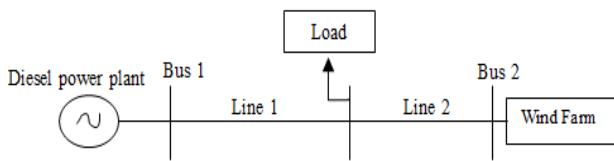


**Fig. 5.** Studied system for wind farm power fluctuations impact on electrical grid frequency illustration.

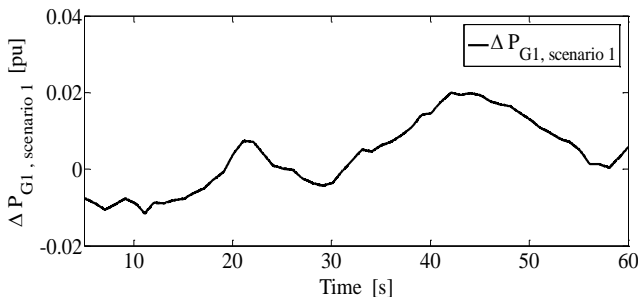


**Fig. 6.** Diesel power plant contribution to control frequency.

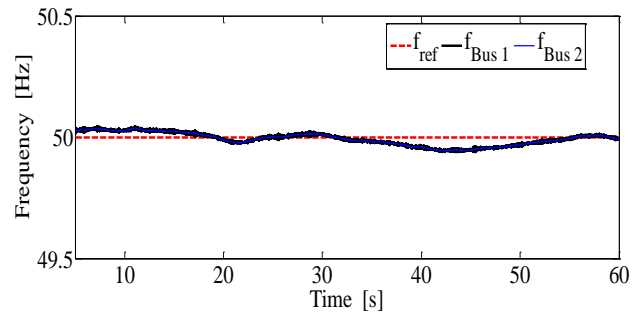


**Fig. 7.** Frequency in the Bus 1 and Bus 2.

Figure 6 shows the power supplied by the diesel plant to compensate the electrical grid’s frequency variations caused the offshore wind farm production. The grid frequency is kept constant at 50 Hz as illustrated in Fig.7. This control is obtained by using the first reserve of power at the diesel plant, whereas the first reserve should be used to correct the gap between production and consumption to improve the electrical grid stability. To avoid these additional constraints for electrical grid, the wind farm contribution must be adapted to grid code requirements. In this paper, the requirements are focused on energy quality and power gradient  $(dP/dt)_{limit}$ . These limits are fixed through electrical grid codes which are not same for all countries. For example, the power gradient limits fixed by electrical grid managers in Germany, Denmark and Nordic Grid Code are shown in Table 3.

**Table 3.** Power gradient limits extracted in [2], [7] and [8].

Grid code	Power gradient $(dP/dt)_{limit}$
E-on, Germany	10% of $P_{nom}$ per minute
Eltra, Denmark	10-100% of $P_{nom}$ per minute
Nordic Grid Code	10% of $P_{nom}$ per minute

To verify if the power from wind farm is compatible to grid code requirement, the ratio expressed in (7) is used, where  $r$  presents 10% of rated power (0.5MW/s), and  $\tau_r$  is the sampling time in [s].

$$r = \frac{P_p(t + \tau_r) - P_p(t)}{\tau_r} \tag{7}$$

This equation is used to estimate the required power  $P_r$  profile for electrical grid using wind farm production  $P_p$ . The resulting profile which corresponds to grid code requirement is presented in Fig.8.

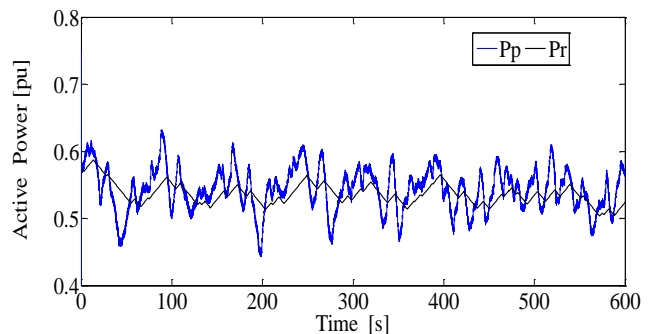


**Fig. 8.** Active power  $P_p$  and  $P_r$ .

Figure 8 shows that, the wind farm production  $P_p$  has more fluctuations compared to required power  $P_r$  for electrical grid. The difference between  $P_p$  and  $P_r$  must be compensated by energy storage device so that, the assigned energy to electrical grid becomes compatible to grid code requirements.

**5. Energy storage devices to smooth the wind farm production**

Used method to choose energy storage device for the wind farm production mitigation so that it becomes compatible to grid code requirements is based in two criteria. These last one including the dynamics of energy storage device (time response) and the autonomy. The power reference destined to energy storage device is presented in Fig.9. This reference is obtained from the difference between  $P_r$  and  $P_p$ .

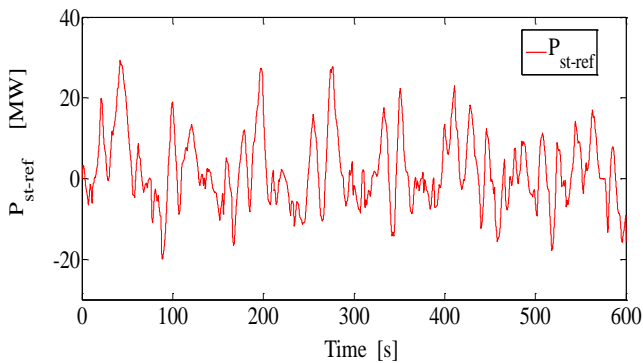


**Fig. 9.** Power reference for energy storage unit.

The reference power profile given in Fig.9 is used to determine the most appropriate storage devices. The first step is to analyze the spectrum of this power, to determine the necessary dynamic of system. The second step is to locate the maximum power and maximum energy in profile.

The spectral analysis of the power reference  $P_{ts-ref}$  is illustrated in Fig.10. This spectrum allows highlighting the different dynamics or existing frequencies. These frequencies are compared with the frequencies which characterizing each energy storage unit given by Ragone plot illustrated in Fig.11.

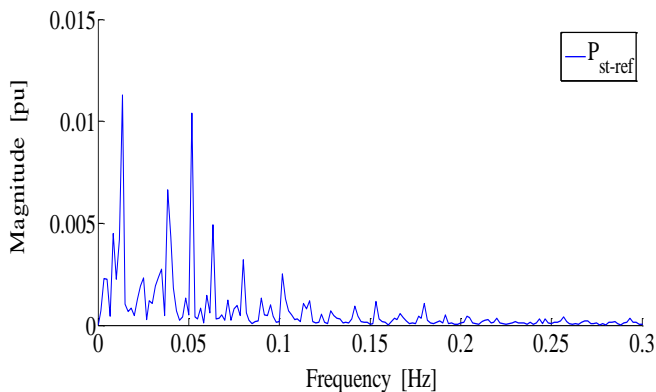


**Fig. 10.** Energy storage device power reference spectrum analysis.

According to spectral analysis, the majority of the harmonics have frequencies that correspond to those of the two zones, namely the low and medium frequencies. The average frequencies are below 0.01Hz, and low frequencies are included between 0.01 and 0.3 Hz. All storage units can be characterized by a relationship of energy-power type, this characteristic can be presented in Ragone diagram as shown in Fig.11 [23].

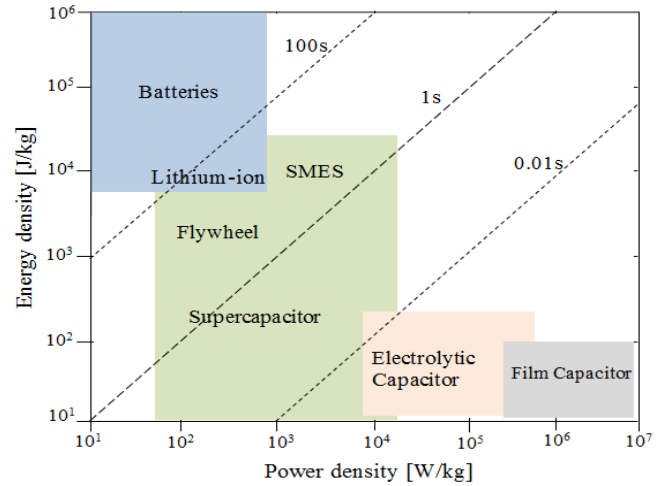


**Fig. 11.** Ragone diagram.

The energy density and specific energy characterizes the ability of energy storage unit to store energy. The power density characterizes the ability to accumulate or make available instantly an amount of energy. This behavior allows to classified the energy storage units based, skills on the given time horizons, which corresponding to their Good Reaction Time (GRT) [24]. In Fig.11, the batteries have a GRT superior than 100s, for the majority of the batteries with an exception for few and lithium batteries which can work up to 3.6s. Flywheels, superconductors and supercapacitors have a GRT between one hundredth and one hundred seconds. Electrolyte capacitors or plastic film have a GRT between the micro and millisecond.

The comparison between the existing frequencies in the power reference spectral and those characterize each storage unit shows that, four energy storage devices can be candidate, namely, the lithium-batteries, the supercapacitors, the flywheels and SMES. In order to make a choice among these technologies, the maximum power and energy in profile can be computed.

The main variables which characterize the energy storage devices are the maximum power and the maximum energy which can be supplied by energy storage unit during the charge and discharge operations. On the curves of the reference power, the maximum power that the storage unit must provide is 30 MW and the maximum energy is computed using equation (8).

$$E_{st-ref-max} = \max \left( \int_t P_{st-ref} dt \right) \tag{8}$$

The computed maximum energy is 104.16kWh. Table 4 summarizes the most recent three modules for storage

technologies and their energy characteristics with an exception for the large modules of the SMES which are not yet commercially available, [25]. Regarding the efficiency aspect, the lithium-batteries and supercapacitors are more advantageous than flywheels, however in terms of the life it is the opposite. In our analysis, the efficiency and life time aspects are secondary, because the considered criterions are focused on the power density and energy density for each energy storage devices.

**Table 4.** Basic characteristics of storage units, [26] and [27].

Technology	Efficiency %	Lifetime	Some modules available on the market
lithium-ion Battery	90-95	High nombres of cycles	2MW/ 500 kWh, Source A123 1MW /540kWh, Intensium® Max 20 de Saft
Supercapacitor	90-95	10 years	1MW /2.3kWh. Unités SC modulaire Siemens Sitas SS
flywheel	80-90	20 years	100kW/25kWh , 150kW/12.5kWh Beacon Power, LLC

To determine the number of modules for each energy storage device, two factors are defined as expressed in equations (9) and (10), where  $P_{mod-max}$  is the maximum power of the module and  $E_{mod-max}$  presents the module maximum energy.

$$N_P = \frac{P_{st-ref-max}}{P_{mod-max}} \tag{9}$$

$$N_E = \frac{E_{st-ref-max}}{E_{mod-max}} \tag{10}$$

The first factor is the number of modules required to provide power  $P_{st-ref-max}$  and the second factor is the number of modules required to provide energy  $E_{st-ref-max}$ . Estimated values of  $N_p$  and  $N_E$  are given in Table 5.

**Table 5.** Values of  $N_p$  and  $N_E$ .

Technology	$N_P$	$N_E$
Lithium-ion Battery	15	1
Supercapacitor	15	45
Flywheel	200	9

Table 5 show that, using energy storage based on flywheel device needs 200 modules to satisfy the maximum power and 9 modules for maximum energy requirement. In the case of supercapacitors, the number of modules is 15 to provide power  $P_{st-ref-max}$ ; and 45 modules for Energy  $E_{st-ref-max}$ . The number of modules for lithium-ion batteries is 15 for power; and is 1 for energy. In summary to satisfy both constraints 200 modules of flywheels, or 45 modules of supercapacitors or 15 modules of lithium batteries are necessary. Therefore, the choice is to use lithium batteries, this choice is motivated in part by the reduced number of modules compared to supercapacitors and flywheel technologies.

**6. Energy management based on wind farm production smoothing**

Figure 12 shows the association of the batteries and wind farm in order to smooth the power fluctuations from to be compatible with that requested by the grid code. In the case of an offshore wind farm wind farm, the lithium-battery is used as illustrated in figure.

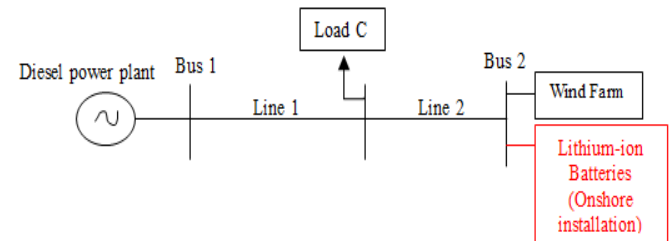


**Fig. 12.** Lithium-battery integration in offshore wind farm

**6.1. Active and reactive power control loops in battery side**

The power reference for battery module is determined using equation (11),  $P_{r-ref}$  is the required power by electrical grid manager, and  $P_p$  is the available power in wind farm.

$$P_{Li-ref} = P_{r-ref} - P_p \tag{11}$$

The power reference estimation for battery module is shown in Fig.13.

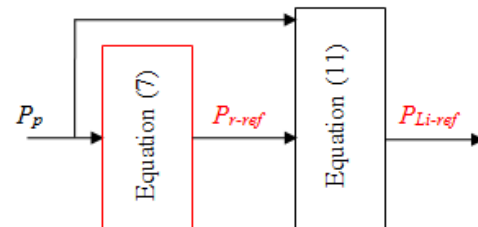


**Fig. 13.** Energy management between the wind park and the equivalent module.

The battery’s power management strategy is illustrated in Fig.14. From the measured voltages and currents at the connection point  $P_{cc}$ , the active and reactive powers are computed. These powers are controlled using proportional-integral regulators through two outer loops, and two inner loops are used to control the currents. To develop an

efficacious control of the power through dq axis currents ( $I_{dst}$  and  $I_{qst}$ ) control. The solution is to synchronize the Park transformation on grid voltage. Thus, when the system is in steady state, the direct component  $V_{dst}$  from the Park transformation is an image of the amplitude of the measured voltage of the grid, and the quadratic component  $V_{qst}$  is equal to zero. This synchronization is achieved by a phase locked loop (PLL) [28]. The model of the battery used is given in [29] and [30].

The wind turbine and PMSG control strategies are based on oriented vector control of stator voltages [28] and [31] as illustrated in Fig. 15. The first role of inverter presented in Fig. 16 is to maintain the DC-bus voltage at constant value. The second role is to control the reactive power exchanged with electrical grid. More information about the control strategy and PI controller parameters computation can be found in [28] and [31]. These control loops are same for all wind turbines in the wind farm.

6.1. Wind turbine and PMSG control strategies

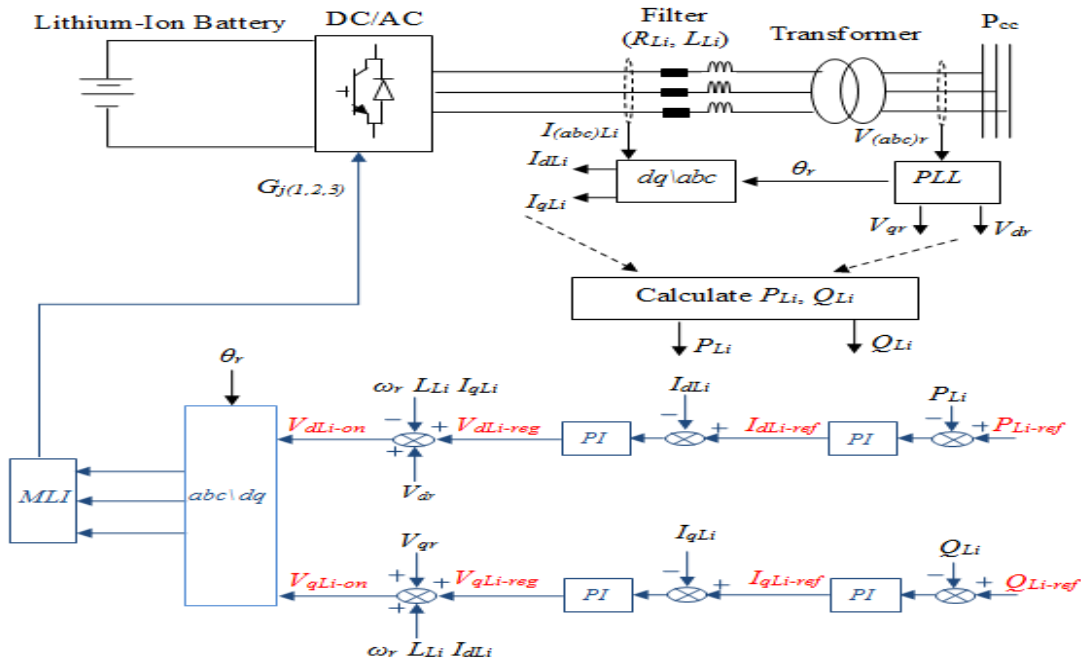


Fig. 14. Battery's energy management.

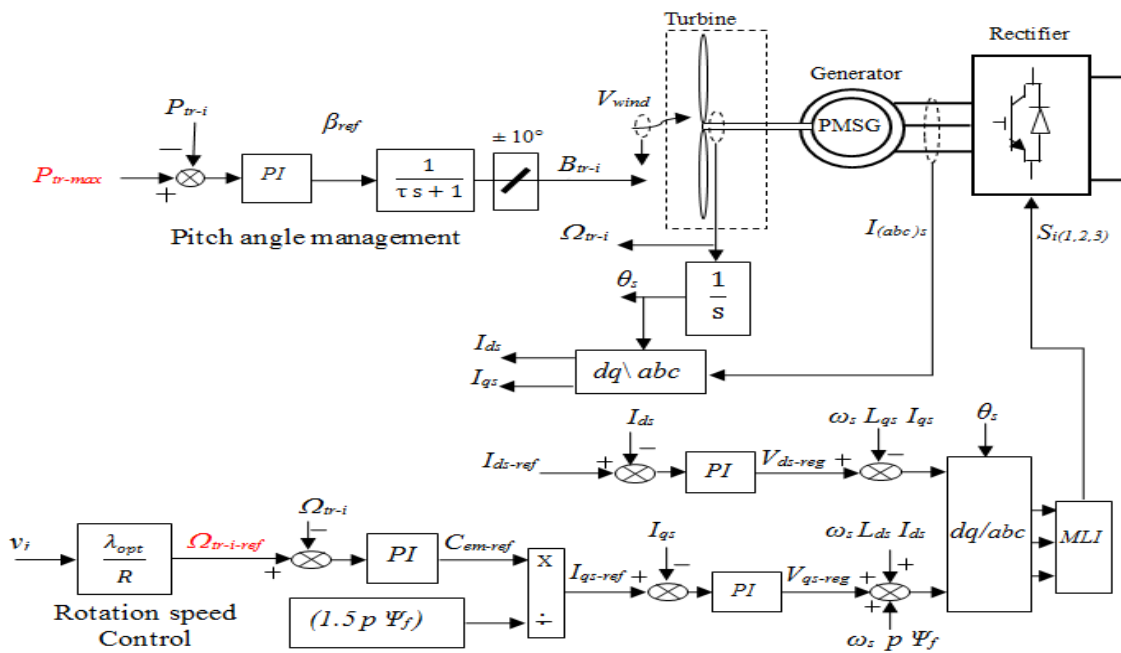


Fig. 15. Wind turbine and PMSG control strategies.

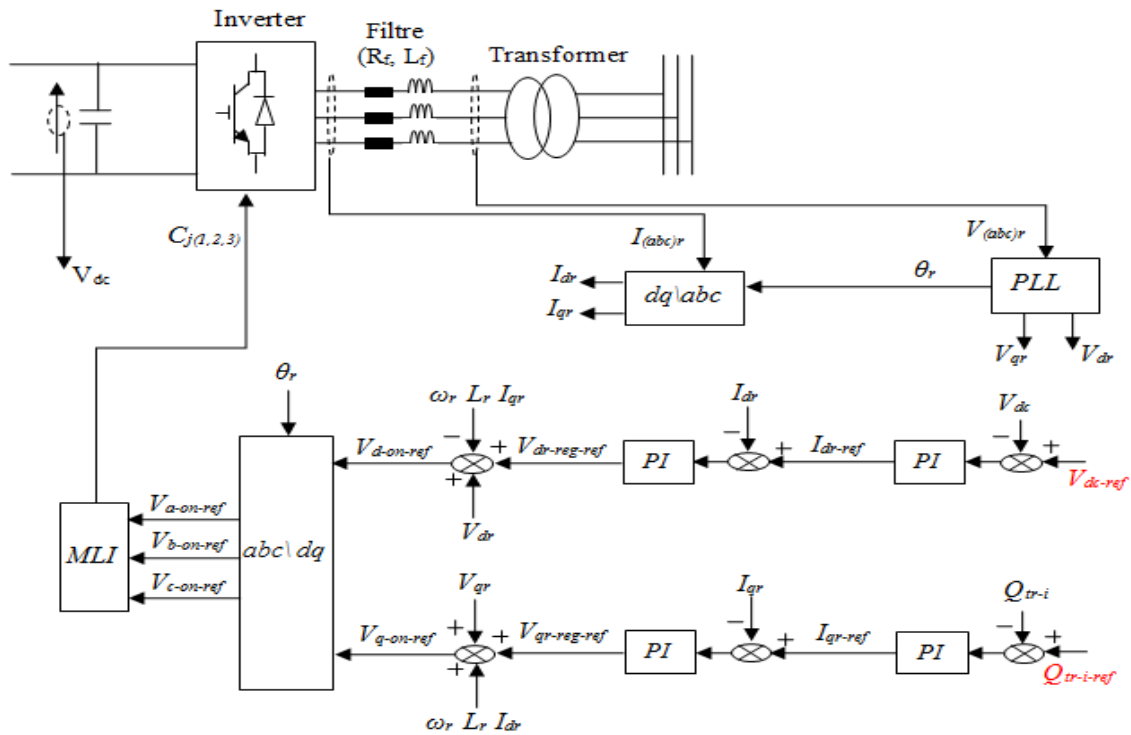


Fig. 16. Energy management method between wind farm and electrical grid.

7. Results and Discussion

The results shown below were obtained by the simulation of the association of the offshore wind farm and lithium-battery. The configuration of the studied system developed in Matlab Simpower system environment is presented in Fig.17. The simulation parameters are given in appendix section.

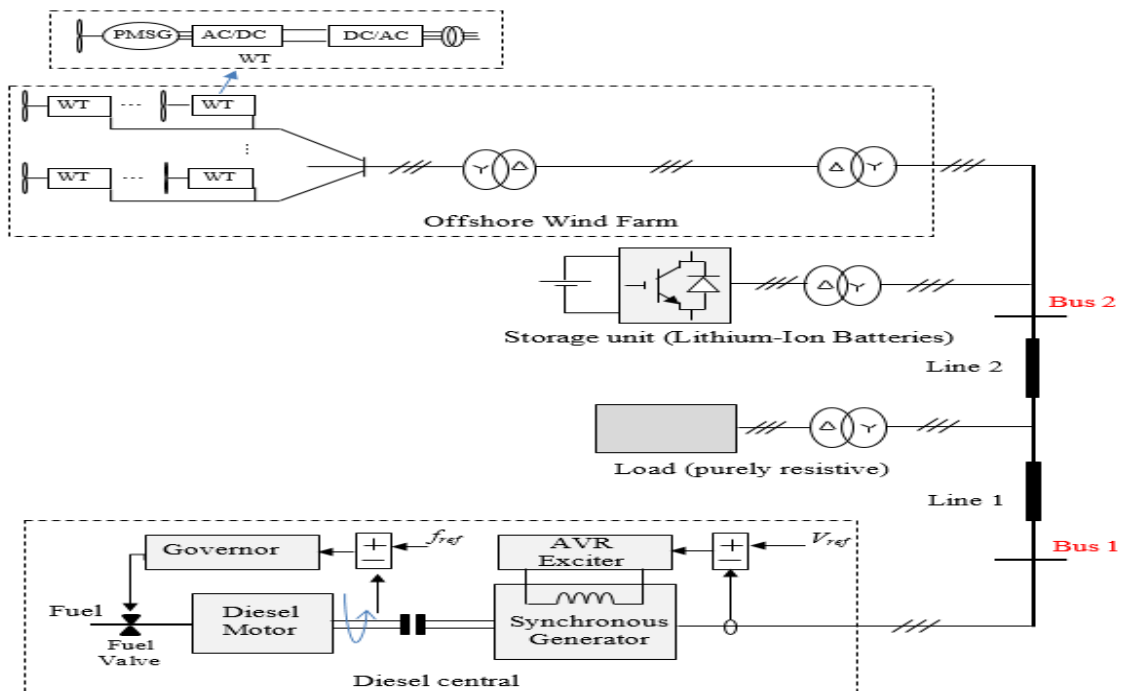
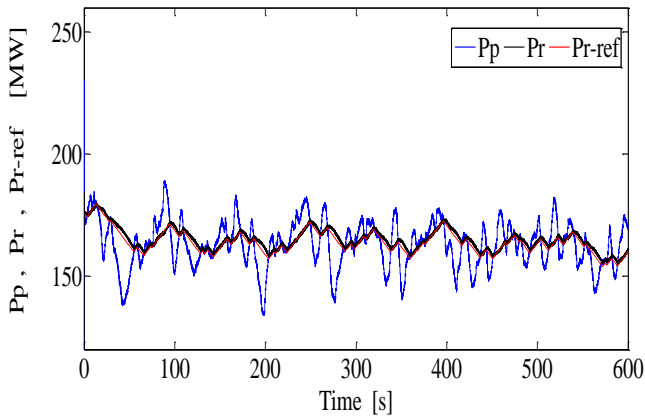


Fig. 17. Studied system configuration.

Using the battery to smooth the power fluctuations is an interesting solution as shown in Fig.18, where the power injected into the grid follows perfectly its reference.



**Fig. 18.** Wind farm production  $P_p$  compared to injected power in grid  $P_r$ .

Measured frequencies on Bus 1 and Bus 2 are maintained at their references (50Hz) as illustrated in Fig. 19. This is assured by the integrated control in the diesel power plant presented in Fig.17, the required power from diesel change according to frequency variations, where  $\Delta P_{G1}$  presented in Fig.20 is estimated from frequency control loop showed in appendix section.

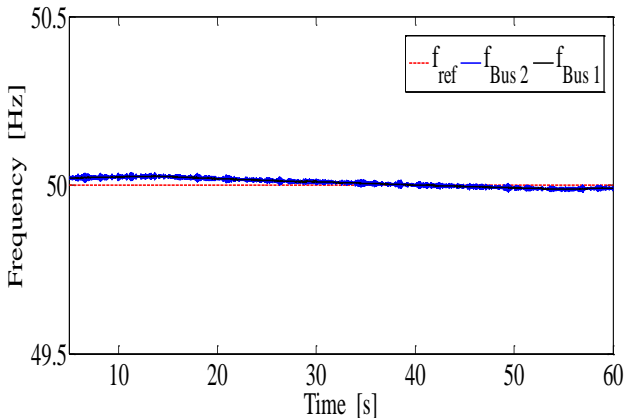


**Fig. 19.** Frequencies in Bus 1 and Bus 2.

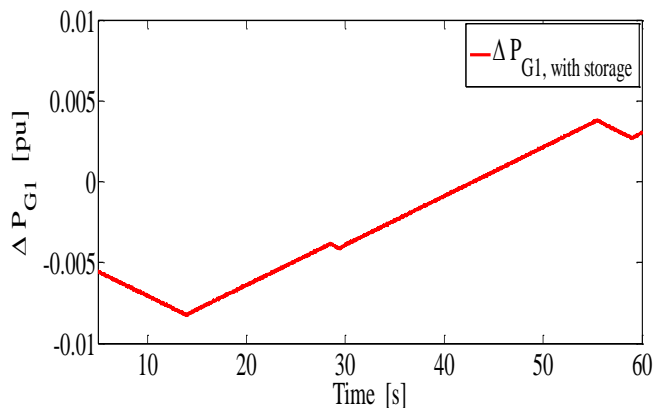


**Fig. 20.** Estimated power from the diesel generator frequency control.

To highlight another major advantage of the battery module integration, a comparison between the estimated power  $\Delta P_{G1}$  from frequency control loop in cases using and without using battery are illustrated in Fig.21. In the case when the battery is used, the maximum value of estimated power  $\Delta P_{G1}$  is about 0.005% of nominal power of the diesel power plant. If the battery module is not used, the maximum value is approximately 0.02% of nominal power of the diesel power plant. In other terms, the estimated power when the battery is used presents a low power compared to that estimated without the battery.

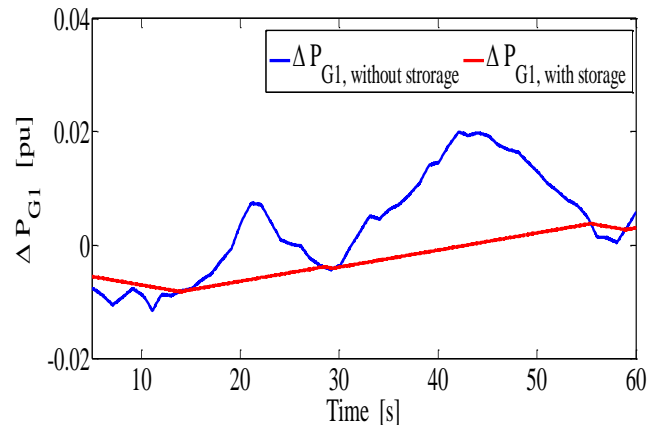


**Fig. 21.** Estimated power from the Diesel generator frequency control when the storage unit is used compared to without using battery.

The wind farm produced power smoothing strategy consists to assign to lithium battery, the all fluctuations of wind generation that exceed the threshold of 10% of the rated power per minute ( $\pm 30\text{MW}/\text{minute}$ ). The contribution of the battery based this control strategy is shown in Fig.22. In order to see that the lithium battery operates in adapted frequency domain, the lithium battery power spectrum is presented in Fig.23. According to spectral analysis, the existing dynamics are almost zero for the frequencies exceeding 0.27 Hz. This threshold corresponds to usually dynamic response domain of the lithium batteries. Based on these results the smoothing mission of wind production does not degrade the lithium batteries.

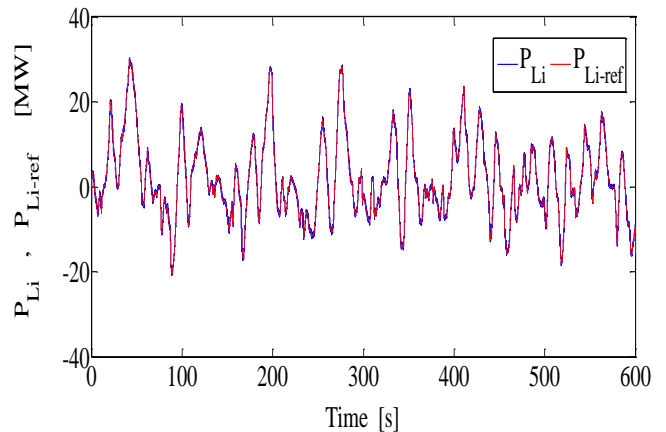


**Fig. 22.** Contribution of the lithium battery.

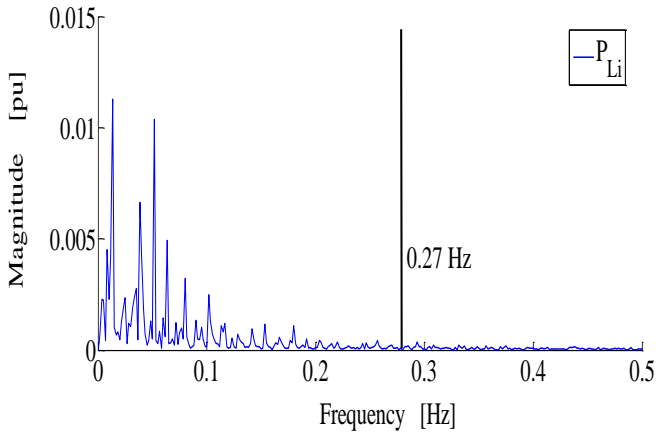


**Fig. 23.** Lithium battery power spectral analysis.

Figure 24 shows the measured currents in AC Bus 2. It is observed that the injected current in the grid has fewer fluctuations compared to that produced by the wind farm, because the power fluctuations are mitigate by the battery. The zoomed section of the currents measured in AC-Bus 2 is plotted in Fig.25, where the frequency of the currents is about 50 Hz.

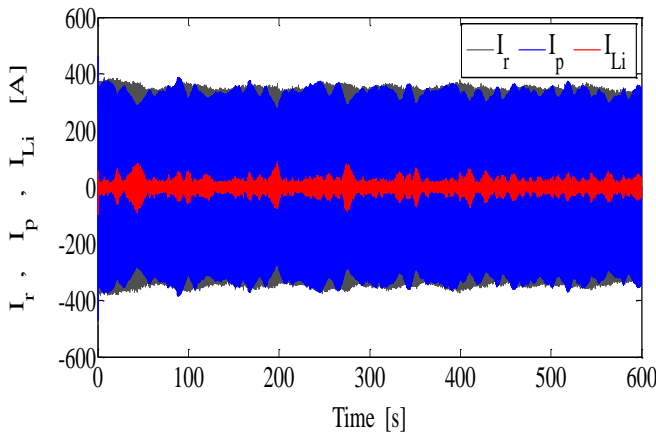


**Fig. 24.**  $I_r$  presents the injected current in the grid,  $I_p$  is the current from the wind farm, and  $I_{Li}$  correspond to current of the lithium battery.

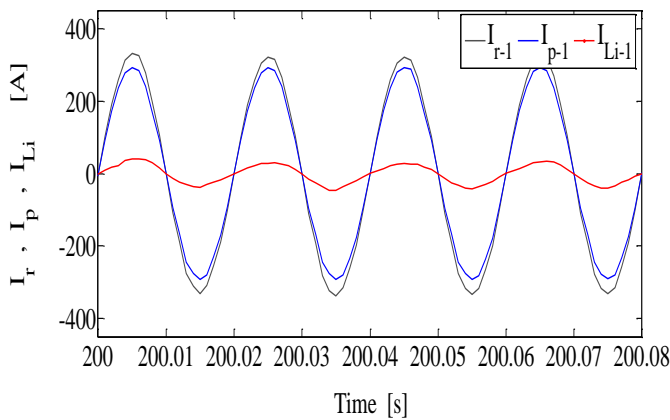


**Fig.25.** Zoom of the currents in AC Bus2.

The battery terminal voltage and current are respectively shown in Figures 26 and 27. That of the battery state of

charge (SOC) is presented in Fig.28. The battery current presents the same fluctuations to that of the power as illustrated in Fig.22. This is logical because its voltage is constant despite changes in its state of charge. This result show the benefits of using DC / AC converter directly to connect the lithium battery to the grid without using classical DC / DC converters to control the DC-bus voltage applied to the inverter.

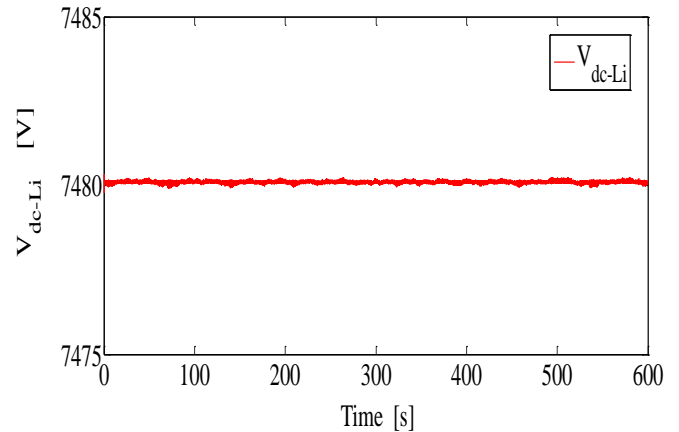


**Fig. 26.** Battery voltage.

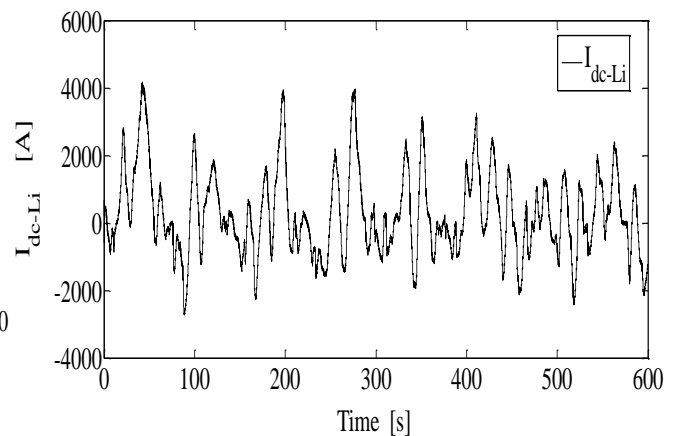


**Fig.27.** Battery current.

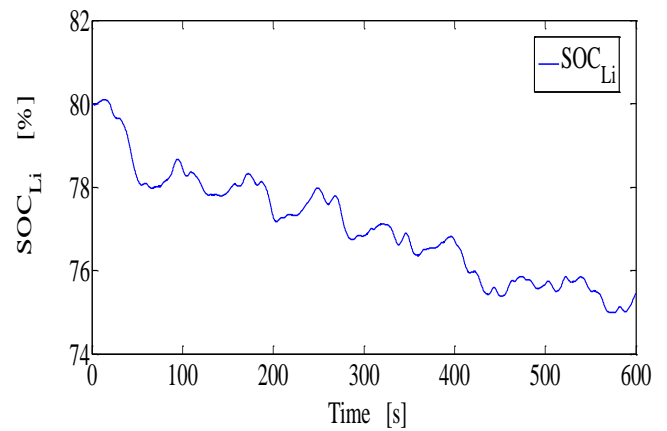


**Fig.28.** Battery SOC.

## 8. Conclusion

This paper presents the analysis of the storage unit's contribution in the wind energy fluctuations compensation for injected power in electrical grid quality improvement. The goal of this analysis is to have a general idea about the ability of different storage technologies to smooth power fluctuations. The result of this analysis shows that there are four technologies of storage units that are candidates for this task; namely, the flywheels, the supercapacitors, the superconductors and the batteries.

An adapted methodology for storage units choosing is proposed, where the results show that the lithium-Ion batteries are well suited for power smoothing mission. The results obtained with the lithium-Ion batteries confirm the performances of the battery to improve the quality of the power injected in the electrical grid, without the battery performances are not degraded.

An additional advantage of using lithium batteries compared to other storage units is due to its high specific capacity. This not only helps to smooth the power but also to make other services such as improving the impact of poor forecasting.

## References

- [1] T.R. Ayodele, A.A. Jimoh, J.L Munda, J.T Agee," Challenges of Grid Integration of Wind Power on Power System Grid Integrity: A Review", International journal of renewable energy research (IJRER), Vol.2, No.4, 2012
- [2] Sourkounis and P. Tourou, "Grid Code Requirements for Wind Power Integration in Europe", Conference Papers in Energy, Vol. 2013, pp. 19–27, 2013
- [3] Gestionnaire du Réseau Transport d'électricité, " RTE met en service un nouveau dispositif de prévision de l'énergie éolienne et photovoltaïque: Le réseau électrique, vecteur du développement des énergies renouvelables ", Press pack. Novembre 2009.
- [4] Thomas ACKERMANN," Wind Power in Power Systems ", Royal Institute of technology, Wiley, 2005.
- [5] Adrien COURBOIS," Étude expérimentale du comportement dynamique d'une éolienne offshore flottante soumise à l'action conjuguée de la houle et du vent ", PhD dissertation, École Centrale de Nantes, Avril 2013.
- [6] Ministry of Ecology, "Sustainable Development and Energy Wind power and photovoltaics: energy issues, industrial and societal (in French)", Technical Report, September 2012.
- [7] M. Tsili and S. Papathanassiou," A review of grid code technical requirements for wind farms", IET Renewable Power Generation, Vol. 3, No.3, pp. 308–332. September 2009.
- [8] A. H. Kassem, El-Saadany E.F, El-Tamaly H.H. and Wahab M.A.A. ,"Ramp rate control and voltage regulation for grid directly connected wind turbines", Power and Energy Society General Meeting - Conversion and Delivery of Electrical Energy in the 21st Century, 2008 IEEE, July 20-24, Pittsburgh, PA, USA 2008.
- [9] I. Pineda, S. Azau, J. Moccia and J. Wilkes," Wind in power 2013: European statistics", European Wind Energy Association (EWEA), technical report, February 2014.
- [10] M. Swierczynski, R. Teodorescu, C. N. Rasmussen, P. Rodriguez and H. Vikelgaard, "Overview of the energy storage systems for wind power integration enhancement", Proc. IEEE ISIE, pp.3749 -3756, 2010.
- [11] S.G Jamdade, P.G Jamdade," Analysis of Wind Speed Data for Four Locations in Ireland based on Weibull Distribution's Linear Regression Model", International Journal of Renewable Energy Research, IJRER, Vol.2, No.3, 2012.
- [12] X. Han, J. Guo, P. Wang, and Y. Jia, " Adequacy study of wind farms considering reliability and wake effect of WTGs", Power and Energy Society General Meeting, 2011 IEEE, July 24-29, San Diego, USA, 2011.
- [13] Jinkyoo Park, Kincho H. Law, " Cooperative wind turbine control for maximizing wind farm power using sequential convex programming", Energy Conversion and Management, Vol. 101, No. 1, pp.295–316, September 2015.
- [14] H. K. Vladislav Akhmatov, "An aggregate model of a grid-connected, large-scale, offshore wind farm for power stability investigations - importance of windmill mechanical system", International Journal of Electrical Power & Energy Systems, Vol. 24, No.9, pp. 709-717, 2002.
- [15] Cosmin E. Bănceanu, Iulian V, " Coordinated control of wind turbines", Master thesis, Department of Energy Technology - Pontoppidanstræde 101, Aalborg University, Denmark, June 2011.
- [16] Wei Li, G. Joos and C. Abbey, " Wind power impact on system frequency deviation and an ESS based power filtering algorithm solution", IEEE Power Systems Conference and Exposition, PSCE '06, 2006 IEEE PES, , October 29 -November 1, Atlanta GA, USA, 2006.
- [17] Nikos Ath. Kallioras, Nikos D. Lagaros, Matthew G. Karlaftis, Paraskevi Pachy, " Optimum layout design of onshore wind farms considering stochastic loading", Advances in Engineering Software, Vol. 88, pp. 8–20, 2015.
- [18] E. Spahić and G. Balzer, "The Impact of the Wind Farm Size on the Power Output Fluctuation", European Wind Energy Conference (EWEC), Athens, Greece, February 2006.
- [19] M. Jannati, S.H.Hosseinian, B.Vahidi, Guo-JieLi, " A survey on energy storage resources configurations in order to propose an optimum configuration for smoothing fluctuations of future large wind power plants", Renewable and Sustainable Energy Reviews, Vol. 29, pp. 158–172, 2014.

[20] P. Kundur, " Power System Stability and Control ", McGraw Hill Inc., 1994.

[21] IEEE Working Group Report, "Hydraulic Turbine and Turbine Control Models for System Dynamic Studies ", Transactions on Power Systems, Vol. 7, No. 1, pp. 167 – 179, February 1992.

[22] IEEE Recommended Practice for Excitation System Models for Power System Stability Studies, IEEE Std. 421.5-1992.

[23] T. Christen and Martin. Carlen, "Theory of ragon plots. Journal on Power Sources", Vol. 91, No. 2, pp. 210-216, December 2000.

[24] M. A. Tankari, M.B. Camara, B. Dakyo, C. Nichita, "Ultracapacitors and Batteries Integration for Power Fluctuations mitigation in Wind-PV-Diesel Hybrid System", International journal of renewable energy research (IJRER), Vol.1, No.2, pp.86-95, 2011.

[25] Arnaud Badel," Superconducting Magnetic Energy Storage using High Temperature Superconductor for Pulse Power Supply ", PhD dissertation, Université de Grenoble, France, September 2010.

[26] Sites constructeurs: www.saftbatteries.com, www.beaconpower.com

[27] Gauthier DELILLE, " Contribution du Stockage à la Gestion Avancée des Systèmes Électriques, Approches Organisationnelles et Technico-économiques dans les Réseaux de Distribution ", PhD dissertation, Ecole centrale de Lille, France, Novembre 2010.

[28] D. Ikni, M.S. Camara, M.B. Camara, B. Dakyo and H. Gualous," Permanent Magnet Synchronous Generators for Large Offshore Wind Farm Connected to Grid - Comparative Study between DC and AC Configurations", International journal of renewable energy research (IJRER), Vol.4, No.2, 2014.

[29] J. Jang, J. Yoho, " Equivalent Circuit Evaluation Method of Lithium Polymer Battery Using Bode Plot and Numerical Analysis ", IEEE Trans Energy Conversion, Vol. 26, No. 1, pp. 290-298, March 2011.

[30] O.O MENG, I.H ALTAS, " Fuzzy logic control for a wind/battery renewable energy production system ", Turkish Journal of Electrical Engineering and Computer , Vol.20, No.2, 2012.

[31] Mohamed Mansour, M. N. Mansouri, M.F. Mmimouni," Study and Control of a Variable-Speed Wind-Energy System Connected to the Grid", International Journal of Renewable Energy Research, IJRER, Vol.1, No.2, pp.96-104, 2011.

[32] B. Sedaghat, A. Jalilvand, R. Noroozian, "Design of a multilevel control strategy for integration of stand-alone wind/diesel system ", Electrical Power and Energy Systems, Vol. 35, pp.123–137, 2012.

Wind farm parameters

Symbol	Value	Name
$P_n$	300 MW	Nominal Power
$V_{Wind Farm-output}$	225 kV	Nominal Voltage

Turbine parameters

Symbol	Value	Name
R	58 m	Turbine blade radius
$J_{tr}$	$10^4$ kg. m <sup>2</sup>	Inertia of wind turbine
$C_{pmax}$	0.53	Maximum power coefficient
$\lambda_{opt}$	6.89	Optimal tip speed ratio
$N_b$	3	Number of blades

PMSG parameters

Symbol	Value	Name
$P_n$	5 MW	Nominal Power
$J_m$	$10^2$ kg. m <sup>2</sup>	Inertia of PMSG
$\Omega_{tr}$	13 rpm	Rotor rated speed
$R_s$	6.25 mΩ	Stator resistance
$L_s$	4.229 mH	Self-inductance
$\Psi_f$	11 Wb	Permanent magnetic flux
p	75	Number of pole pairs
$V_{dc}$	5 kV	DC bus voltage

Electrical line parameters (Model PI)

Symbol	Value	Name
R1	0.0127 Ω/km	Positive sequence resistance
R0	0.384 Ω /km	Zero sequence resistance
L1	0.937 mH/km	Positive sequence inductance
L2	4.12 mH/km	Zero sequence inductance
C1	12.74 nF/km	Positive sequence capacitance
C2	7.75 nF/km	Zero sequence capacitance
f	50	Frequency

Appendix

Simulation parameters

Onshore and offshore transformer parameters

Symbol	Value	Name
$S_n$	400 MVA	Nominal power
$R_1$	0.681 $\Omega$	Resistance for winding 1
$L_1$	4.12 mH	Inductance for winding 1
$U_1$	33 kV	Nominal voltage for winding 1
$R_2$	0.330 $\Omega$	Resistance for winding 2
$L_2$	0.718 mH	Inductance for winding 2
$U_2$	225 kV	Nominal voltage for winding 2
$R_m$	77801 $\Omega$	Magnetization resistance
$L_m$	206.37 H	Magnetization inductance

Lithium-Ion battery parameters

Symbol	Value	Name
$E_n$	7.48kV	Nominal Voltage
$R_\Omega$	0.2 $\Omega$	Internal Resistance
$I_{bat-nom-d}$	4.01kA	Nominal Discharge Current
$I_{bat-nom}$	1.002kAh	Maximum Capacity

Lithium-Ion battery transformer parameters

Symbol	Value	Name
$S_n$	40 MVA	Nominal power
$R_1$	0.125 $\Omega$	Resistance for winding 1
$L_1$	0.612 mH	Inductance for winding 1
$U_1$	36 kV	Nominal voltage for winding 1
$R_2$	0.050 $\Omega$	Resistance for winding 2
$L_2$	0.3718 mH	Inductance for winding 2
$U_2$	225 kV	Nominal voltage for winding 2

$R_m$	2410 $\Omega$	Magnetization resistance
$L_m$	102.37 H	Magnetization inductance

Main parameters for diesel power plant (more detail in [32])

Symbol	Value	Name
$P_{SM-Nom}$	970 MVA	Nominal Power
$Cos(\varphi)$	0.988	Power Factor
$V_{diesel-output}$	225 kV	Nominal Voltage
$(\Delta P_{G1})_{max}$	10% of $(P_{SM-Nom} \times Cos(\varphi))$	Reserve Power (Primary control)

Load parameters

Symbol	Value	Name
$P_{Load}$	1200 MW	Nominal Power
$V_{Load-output}$	225 kV	Nominal Voltage
$Cos(\varphi)$	1	Power Factor